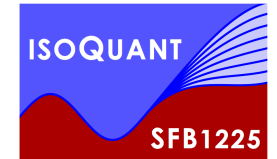




UNIVERSITÄT
HEIDELBERG
ZUKUNFT
SEIT 1386



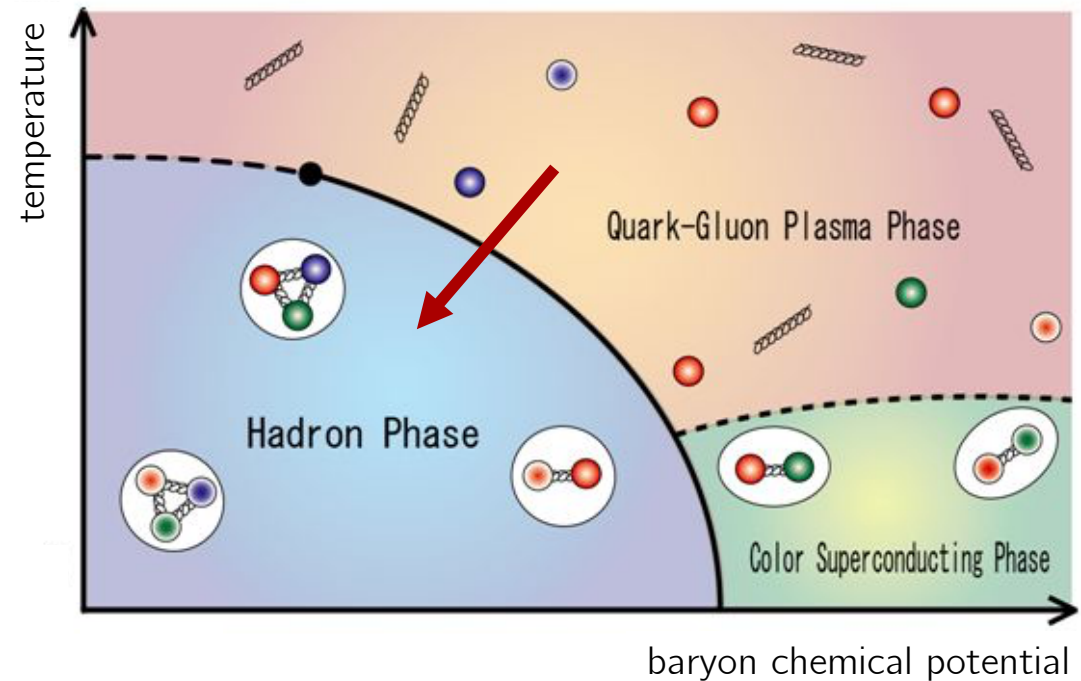
Dynamical Thermalization in the Quark-Meson Model

Linda Shen

Institute for Theoretical Physics, Heidelberg University

with J. Berges, J. Pawłowski, A. Rothkopf

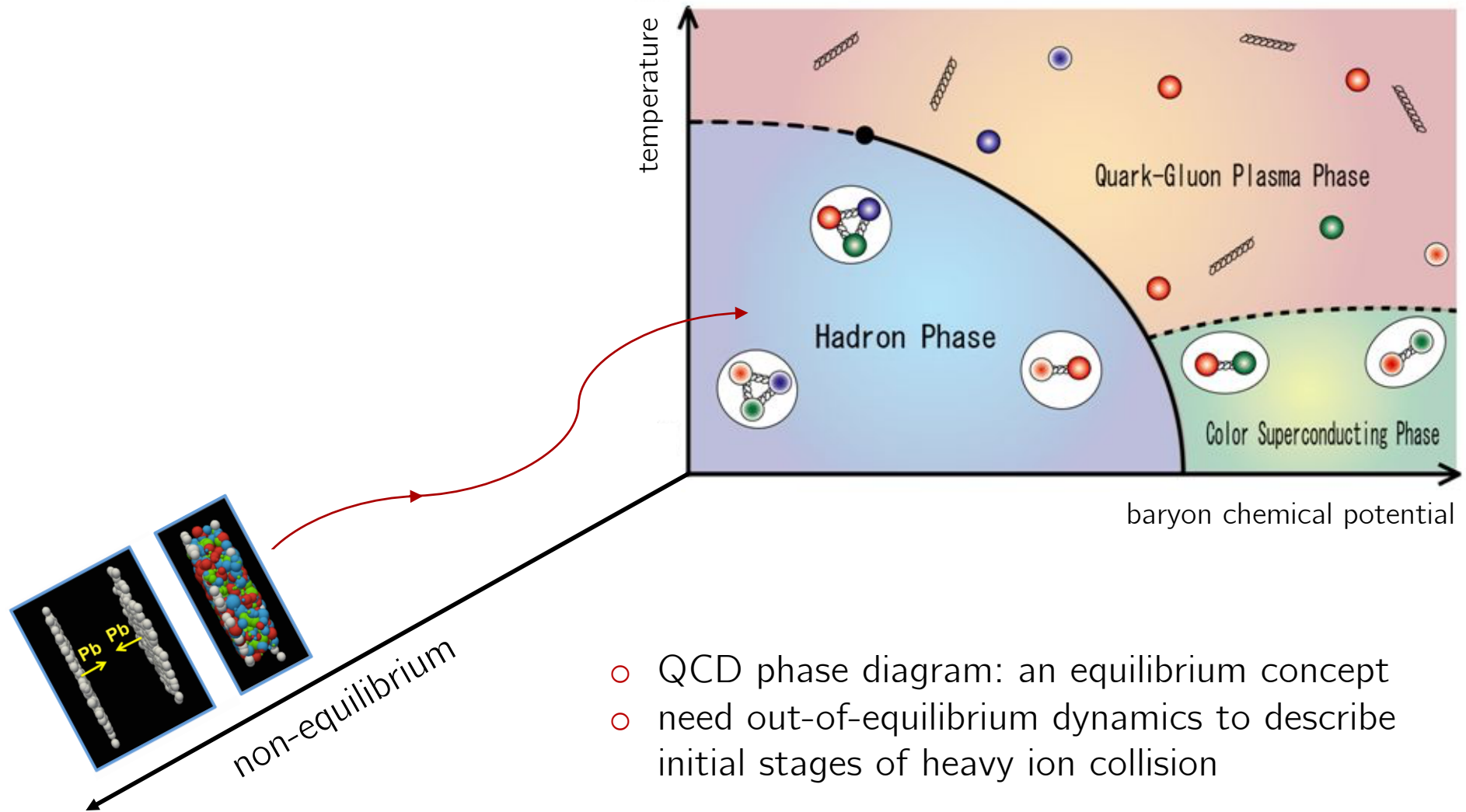
From heavy ion collisions towards the QCD phase diagram: an equilibration process



- QCD phase diagram: an equilibrium concept
- deconfinement + chiral phase transition

Figures from <http://wl33.web.rice.edu/images/HI-cartoon.png>,
http://images.slideplayer.com/25/7893277/slides/slide_3.jpg

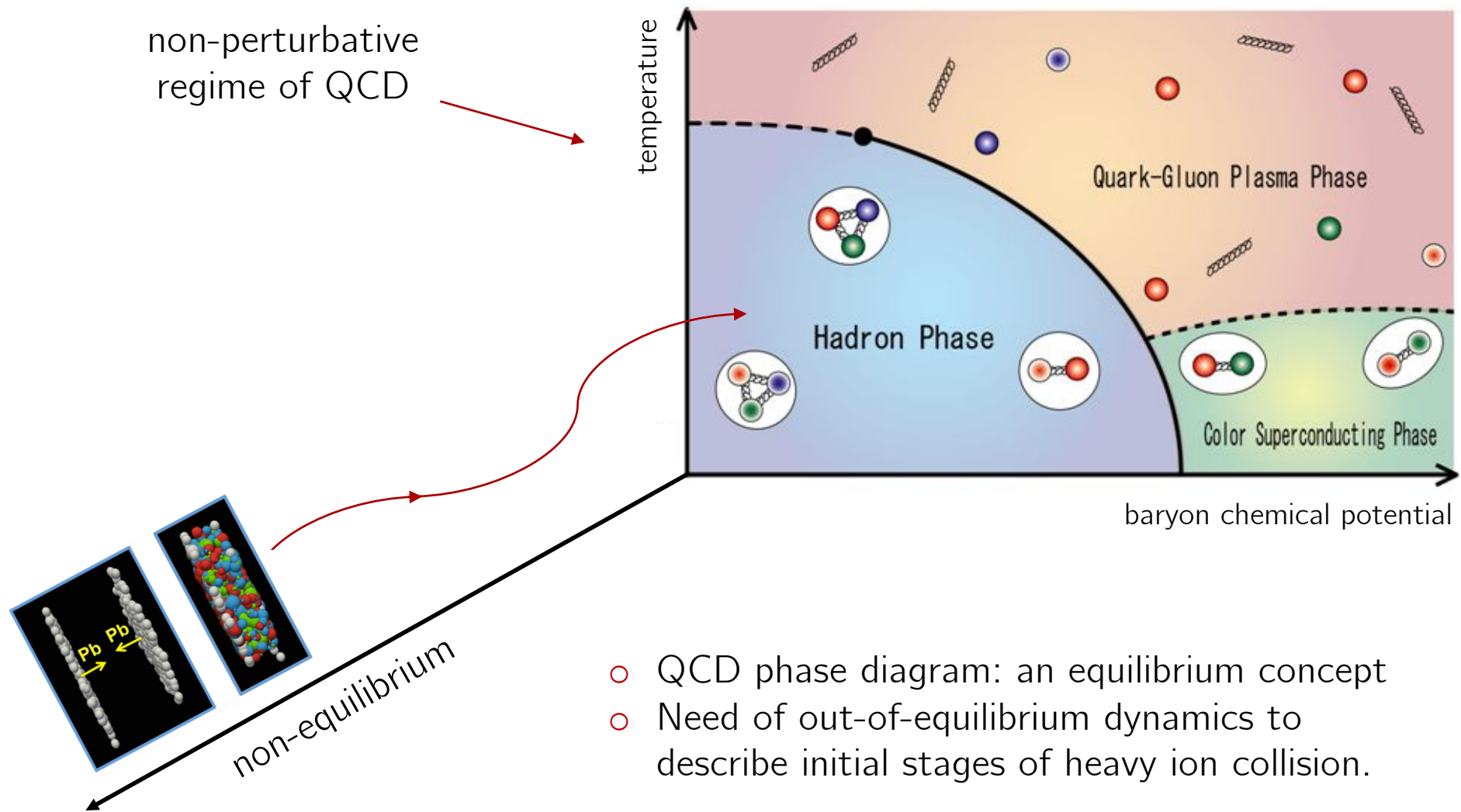
From heavy ion collisions towards the QCD phase diagram: an equilibration process



- QCD phase diagram: an equilibrium concept
- need out-of-equilibrium dynamics to describe initial stages of heavy ion collision

Figures from <http://wl33.web.rice.edu/images/HI-cartoon.png>,
http://images.slideplayer.com/25/7893277/slides/slide_3.jpg

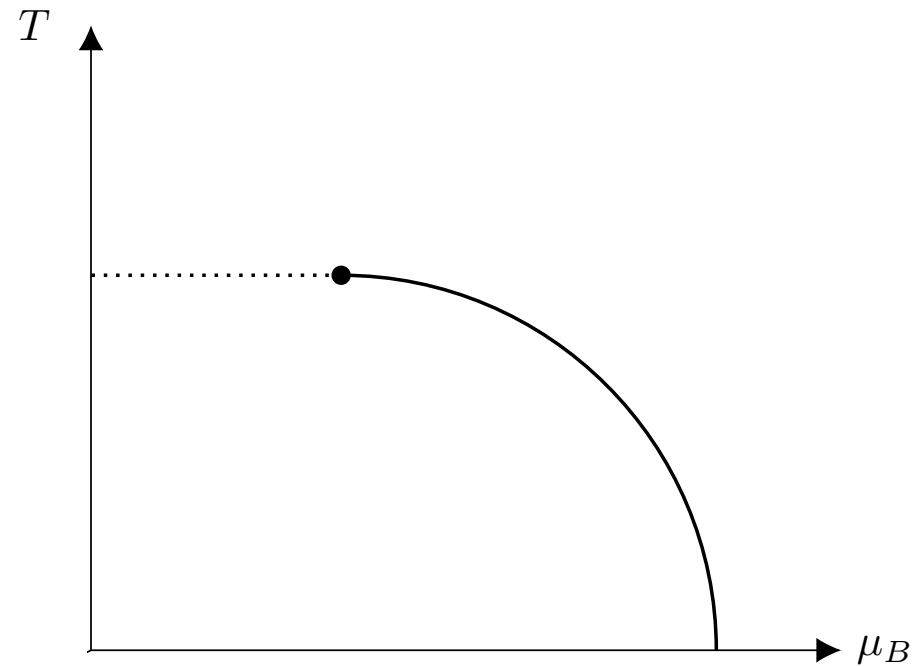
From heavy ion collisions towards the QCD phase diagram: an equilibration process



Figures from <http://wl33.web.rice.edu/images/HI-cartoon.png>,
http://images.slideplayer.com/25/7893277/slides/slide_3.jpg

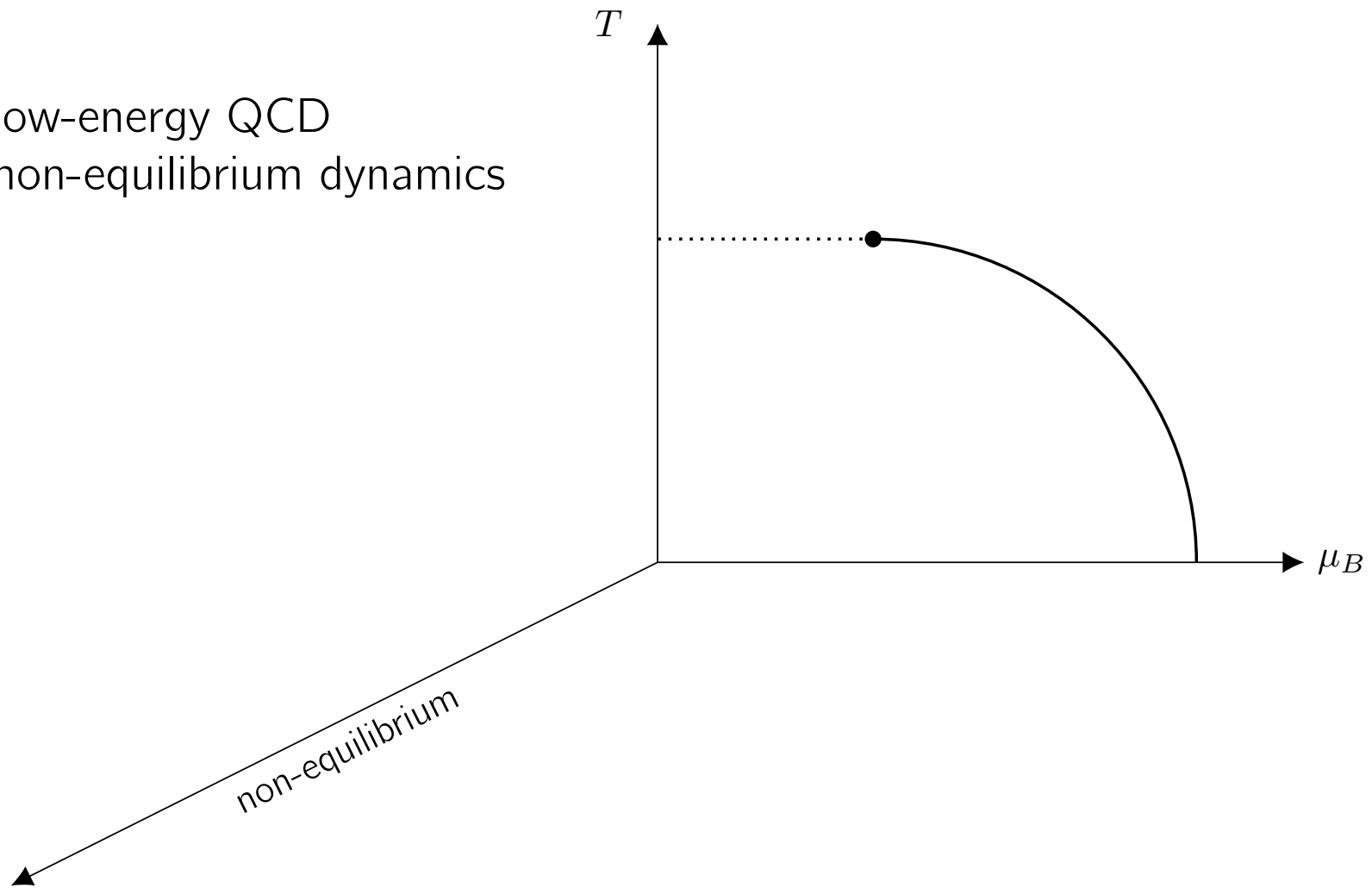
We can investigate this equilibration using effective field theories.

- low-energy QCD



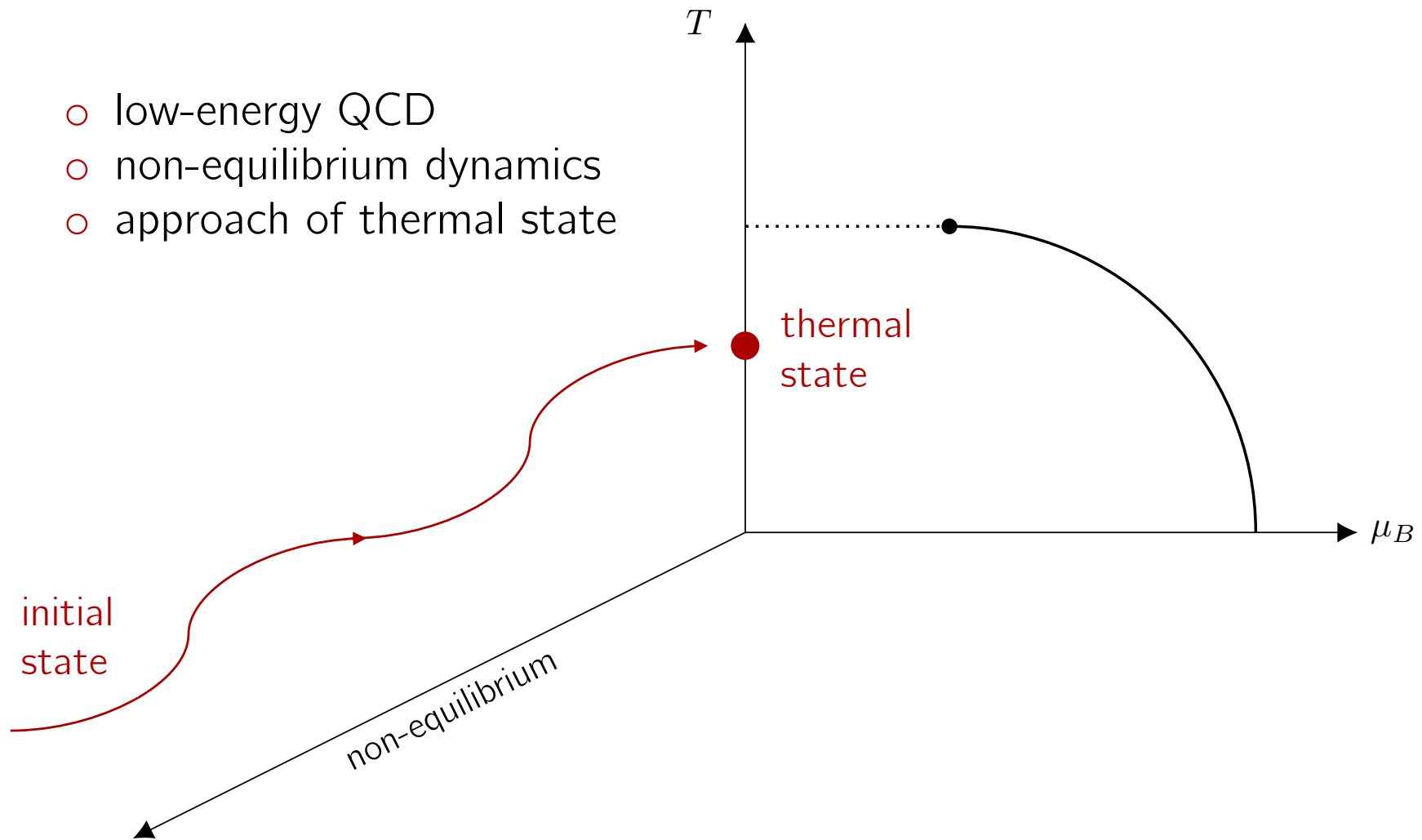
We can investigate this equilibration using effective field theories.

- low-energy QCD
- non-equilibrium dynamics



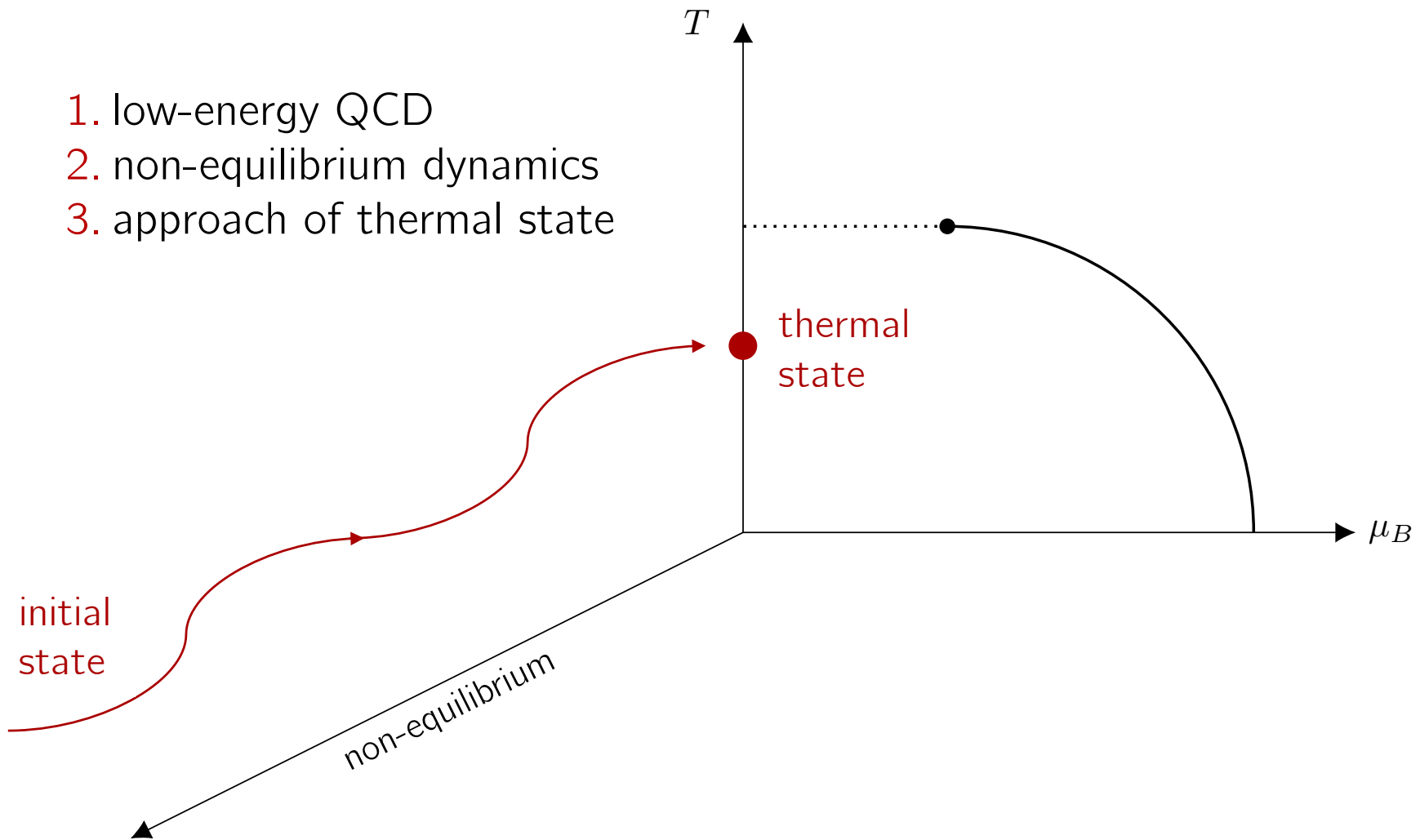
We can investigate this equilibration using effective field theories.

- low-energy QCD
- non-equilibrium dynamics
- approach of thermal state



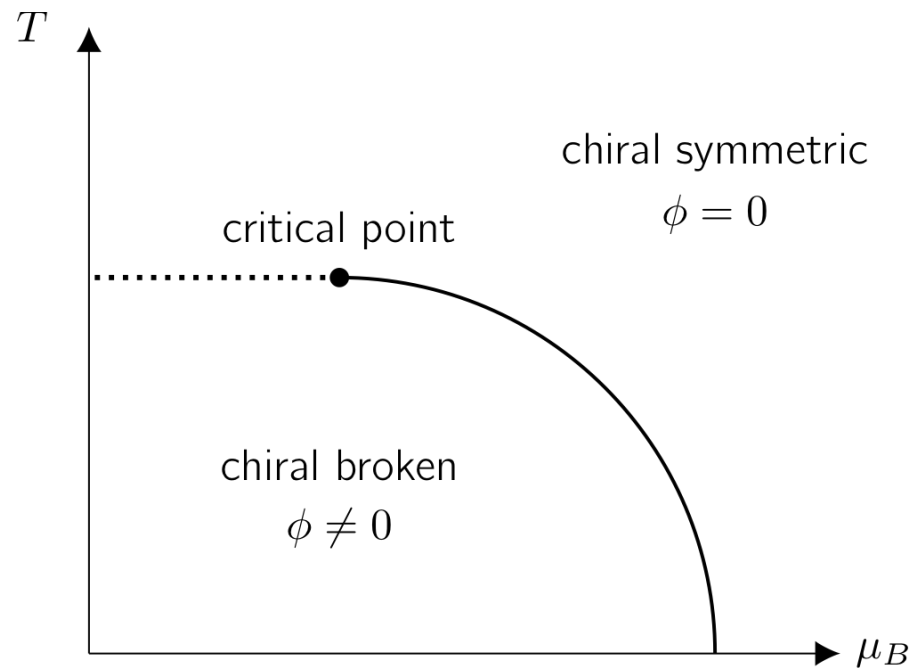
We can investigate this equilibration using effective field theories.

1. low-energy QCD
2. non-equilibrium dynamics
3. approach of thermal state



The quark-meson model provides a successful formulation of QCD below scales ~ 1 GeV.

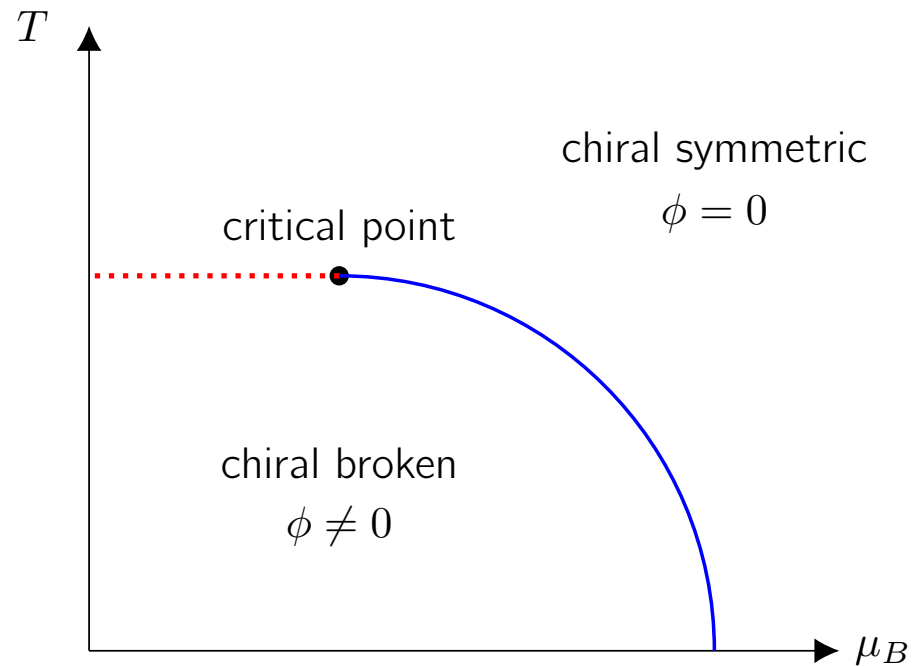
- d.o.f.: light quarks and mesons
- chiral symmetry breaking
- phase diagram with 1st order & 2nd order/crossover transition



Jungnickel, Wetterich. PRD (1996)
Birse. J. Phys. G: Nucl. Part. Phys. (1994)
Petropoulos. J. Phys. G: Nucl. Part. Phys (1998)
Berges, Jungnickel, Wetterich. Int. J. Mod. Phys. A (2003)
Schaefer, Pirner. arXiv nucl-th/9903003 (1999)

The quark-meson model provides a successful formulation of QCD below scales ~ 1 GeV.

- d.o.f.: light quarks and mesons
- chiral symmetry breaking
- phase diagram with 1st order & 2nd order/crossover transition



Jungnickel, Wetterich. PRD (1996)
Birse. J. Phys. G: Nucl. Part. Phys. (1994)
Petropoulos. J. Phys. G: Nucl.Part. Phys (1998)
Berges, Jungnickel, Wetterich. Int. J. Mod. Phys. A (2003)
Schaefer, Pirner. arXiv nucl-th/9903003 (1999)

The quark-meson model provides
a successful formulation of QCD below scales ~ 1 GeV.

$$S[\bar{\psi}, \psi, \sigma, \pi] = \int_x \left[\bar{\psi} [i\gamma^\mu \partial_\mu - m_\psi] \psi - \frac{g}{N_f} \bar{\psi} [\sigma + i\gamma_5 \tau^\alpha \pi^\alpha] \psi \right. \\ \left. + \frac{1}{2} [\partial_\mu \sigma \partial^\mu \sigma + \partial_\mu \pi \partial^\mu \pi] - \frac{1}{2} m^2 [\sigma^2 + \pi^\alpha \pi^\alpha] - \frac{\lambda}{4! N} [\sigma^2 + \pi^\alpha \pi^\alpha]^2 \right]$$

The quark-meson model provides
a successful formulation of QCD below scales ~ 1 GeV.

u & d quark

$$S[\bar{\psi}, \psi, \sigma, \pi] = \int_x \left[\bar{\psi} [i\gamma^\mu \partial_\mu - m_\psi] \psi - \frac{g}{N_f} \bar{\psi} [\sigma + i\gamma_5 \tau^\alpha \pi^\alpha] \psi \right. \\ \left. + \frac{1}{2} [\partial_\mu \sigma \partial^\mu \sigma + \partial_\mu \pi \partial^\mu \pi] - \frac{1}{2} m^2 [\sigma^2 + \pi^\alpha \pi^\alpha] - \frac{\lambda}{4! N} [\sigma^2 + \pi^\alpha \pi^\alpha]^2 \right]$$

The quark-meson model provides
a successful formulation of QCD below scales ~ 1 GeV.

u & d quark

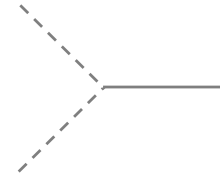
$$S[\bar{\psi}, \psi, \sigma, \pi] = \int_x \left[\bar{\psi} [i\gamma^\mu \partial_\mu - m_\psi] \psi - \frac{g}{N_f} \bar{\psi} [\sigma + i\gamma_5 \tau^\alpha \pi^\alpha] \psi \right. \\ \left. + \frac{1}{2} [\partial_\mu \sigma \partial^\mu \sigma + \partial_\mu \pi \partial^\mu \pi] - \frac{1}{2} m^2 [\sigma^2 + \pi^\alpha \pi^\alpha] - \frac{\lambda}{4! N} [\sigma^2 + \pi^\alpha \pi^\alpha]^2 \right]$$

sigma meson & pions

The quark-meson model provides
a successful formulation of QCD below scales ~ 1 GeV.

u & d quark

Yukawa coupling



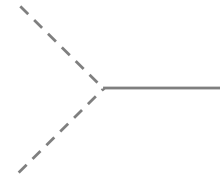
$$S[\bar{\psi}, \psi, \sigma, \pi] = \int_x \left[\bar{\psi} [i\gamma^\mu \partial_\mu - m_\psi] \psi - \frac{g}{N_f} \bar{\psi} [\sigma + i\gamma_5 \tau^\alpha \pi^\alpha] \psi \right. \\ \left. + \frac{1}{2} [\partial_\mu \sigma \partial^\mu \sigma + \partial_\mu \pi \partial^\mu \pi] - \frac{1}{2} m^2 [\sigma^2 + \pi^\alpha \pi^\alpha] - \frac{\lambda}{4!N} [\sigma^2 + \pi^\alpha \pi^\alpha]^2 \right]$$

sigma meson & pions

The quark-meson model provides a successful formulation of QCD below scales ~ 1 GeV.

u & d quark

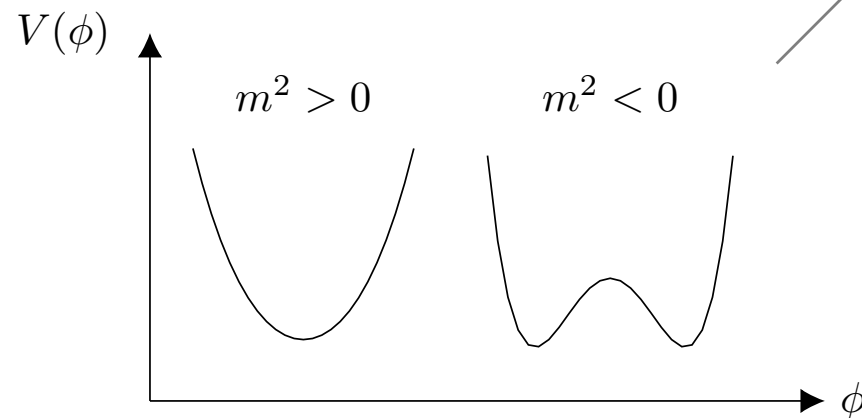
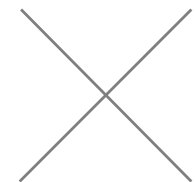
Yukawa coupling



$$S[\bar{\psi}, \psi, \sigma, \pi] = \int_x \left[\bar{\psi} [i\gamma^\mu \partial_\mu - m_\psi] \psi - \frac{g}{N_f} \bar{\psi} [\sigma + i\gamma_5 \tau^\alpha \pi^\alpha] \psi + \frac{1}{2} [\partial_\mu \sigma \partial^\mu \sigma + \partial_\mu \pi \partial^\mu \pi] - \frac{1}{2} m^2 [\sigma^2 + \pi^\alpha \pi^\alpha] - \frac{\lambda}{4!N} [\sigma^2 + \pi^\alpha \pi^\alpha]^2 \right]$$

sigma meson & pions

scalar potential



The 2PI effective action is a practical tool to study thermalization.

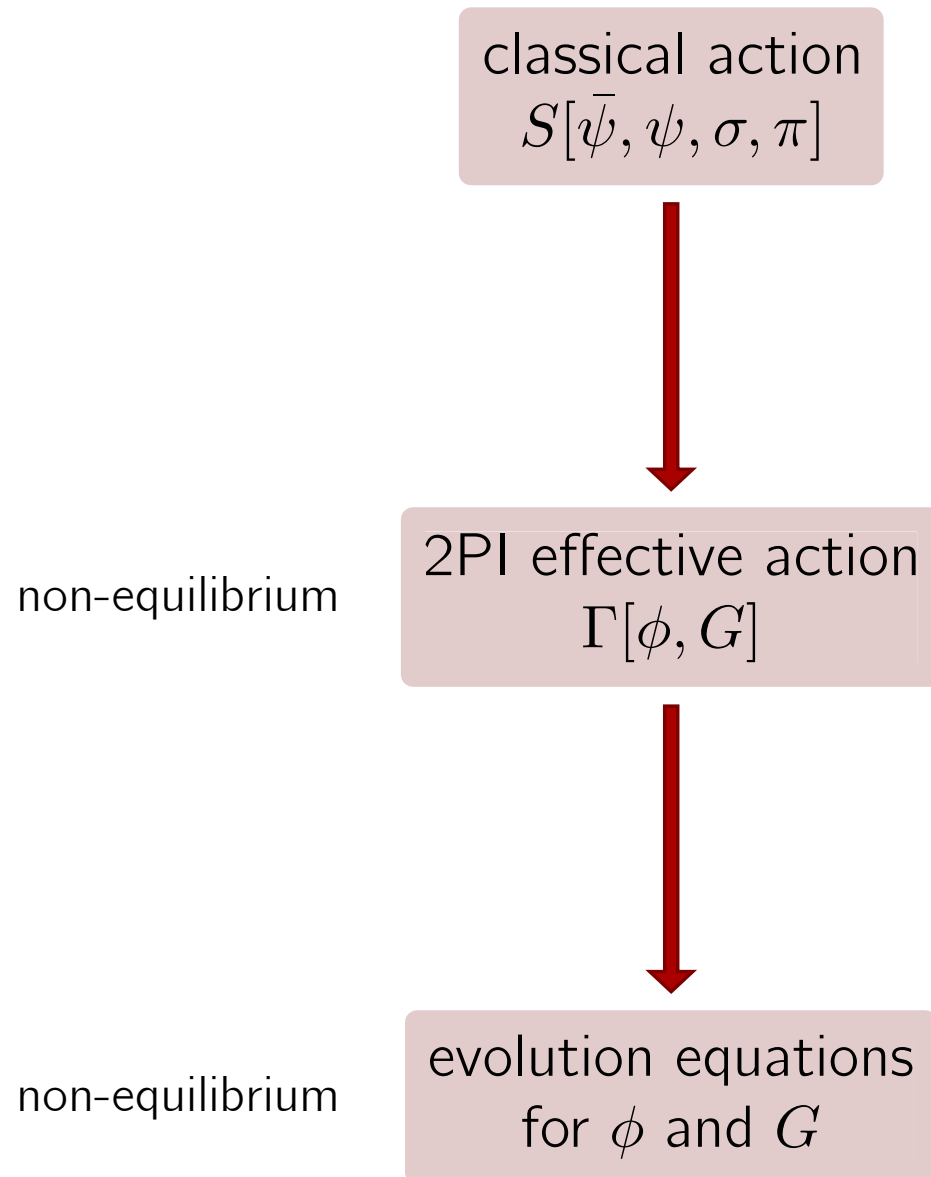
classical action
 $S[\bar{\psi}, \psi, \sigma, \pi]$

Berges. AIP Conference Proc. (2004)
Borsányi. arXiv hep-ph/0512308 (2005)

2PI effective action
 $\Gamma[\phi, G]$

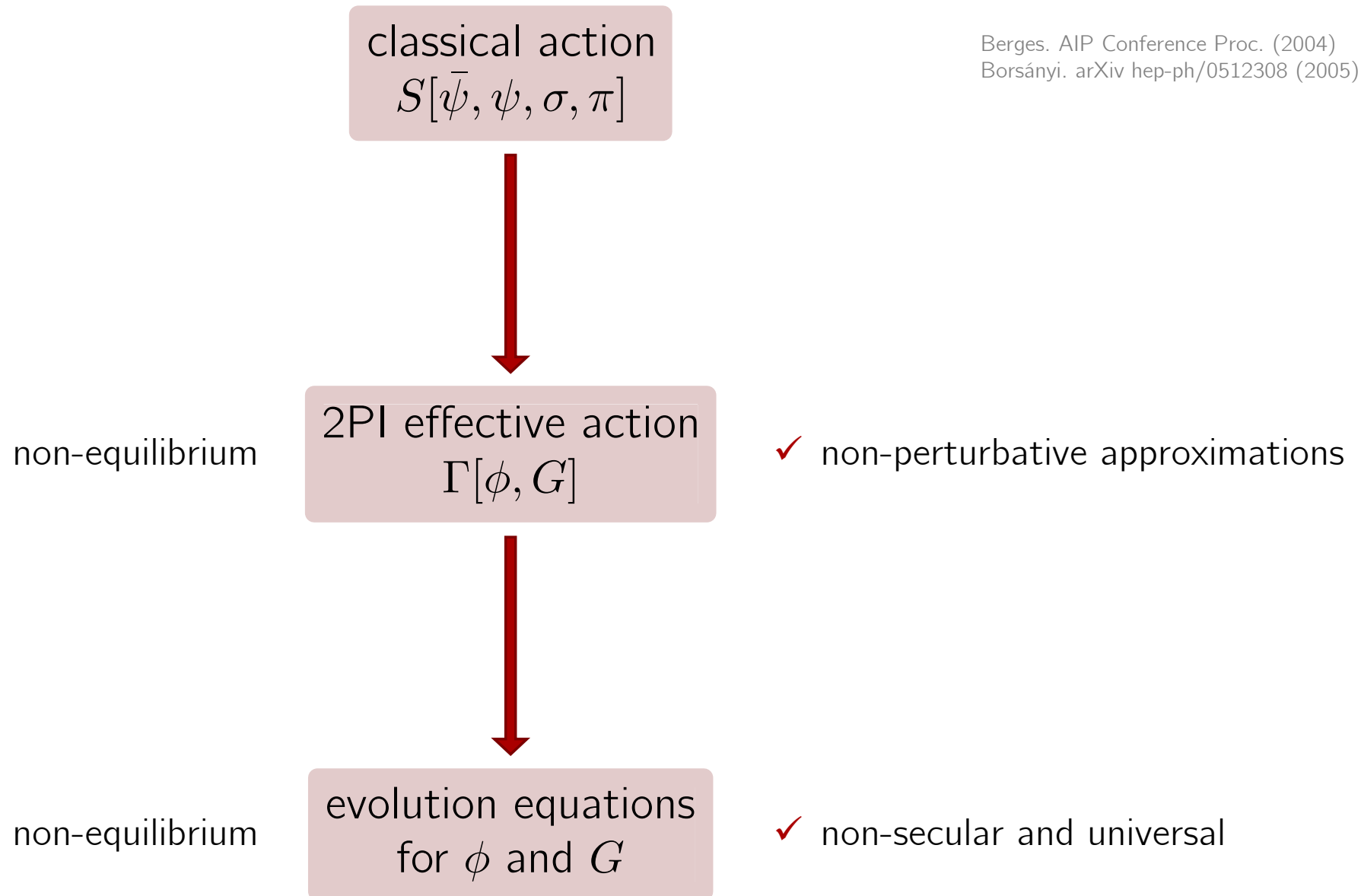
evolution equations
for ϕ and G

The 2PI effective action is a practical tool to study thermalization.



Berges. AIP Conference Proc. (2004)
Borsányi. arXiv hep-ph/0512308 (2005)

The 2PI effective action is a practical tool to study thermalization.



Berges. AIP Conference Proc. (2004)
Borsányi. arXiv hep-ph/0512308 (2005)

classical action
 $S[\bar{\psi}, \psi, \sigma, \pi]$

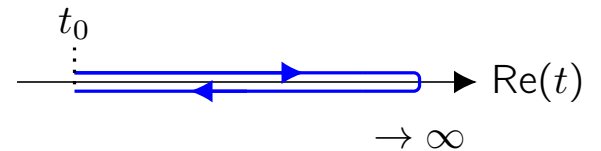
double
Legendre
transf.

2PI effective action
 $\Gamma[\phi, G]$

evolution equations
for ϕ and G

non-equilibrium generating functional for $\rho^{\text{Gauss}}(t_0)$

$$Z[J, R] = e^{iW[J, R]} = \int \mathcal{D}\varphi e^{iS[\varphi] + iJ \cdot \varphi + \frac{i}{2} \varphi \cdot R \cdot \varphi}$$

with 

classical action
 $S[\bar{\psi}, \psi, \sigma, \pi]$

double
Legendre
transf.

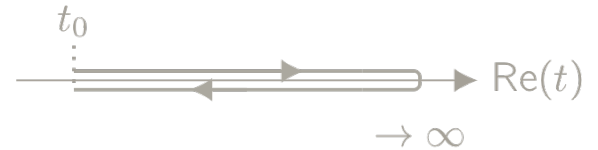
2PI effective action
 $\Gamma[\phi, G]$

stationary
conditions

evolution equations
for ϕ and G

non-equilibrium generating functional for $\rho^{\text{Gauss}}(t_0)$

$$Z[J, R] = e^{iW[J, R]} = \int \mathcal{D}\varphi e^{iS[\varphi] + iJ \cdot \varphi + \frac{i}{2} \varphi \cdot R \cdot \varphi}$$

with 

$$= S[\phi] + \text{1-loop quantum corrections} + \text{2PI diagrams}$$

classical action
 $S[\bar{\psi}, \psi, \sigma, \pi]$

double
Legendre
transf.

2PI effective action
 $\Gamma[\phi, G]$

stationary
conditions

evolution equations
for ϕ and G

non-equilibrium generating functional for $\rho^{\text{Gauss}}(t_0)$

$$Z[J, R] = e^{iW[J, R]} = \int \mathcal{D}\varphi e^{iS[\varphi] + iJ \cdot \varphi + \frac{i}{2} \varphi \cdot R \cdot \varphi}$$

with

$$= S[\phi] + \text{1-loop quantum corrections} + \text{2PI diagrams}$$

large N expansion

$$\underbrace{\text{LO diagrams}}_{\sim N^1} + \underbrace{\text{NLO diagrams}}_{\sim N^0} + \dots + \text{fermion-boson-loop}$$

classical action
 $S[\bar{\psi}, \psi, \sigma, \pi]$

double
Legendre
transf.

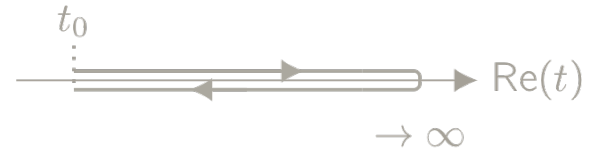
2PI effective action
 $\Gamma[\phi, G]$

stationary
conditions

evolution equations
for ϕ and G

non-equilibrium generating functional for $\rho^{\text{Gauss}}(t_0)$

$$Z[J, R] = e^{iW[J, R]} = \int \mathcal{D}\varphi e^{iS[\varphi] + iJ \cdot \varphi + \frac{i}{2} \varphi \cdot R \cdot \varphi}$$

with 

$$= S[\phi] + \text{1-loop quantum corrections} + \text{2PI diagrams}$$

large N expansion

$$\underbrace{\text{LO diagrams}}_{\sim N^1} + \underbrace{\text{NLO diagrams}}_{\sim N^0} + \dots + \text{fermion-boson-loop}$$

$$[\partial_t^2 + M^2(x; \phi)] \phi(t) = \text{fermion backreaction} + \text{2PI corrections}$$

$$[\square_x + M^2(x; \phi)] G(x, y) = -i \int_z [\underbrace{\Sigma(x, z; \phi, G)}_{\text{self-energy}}] G(z, y) - i\delta(x - y)$$

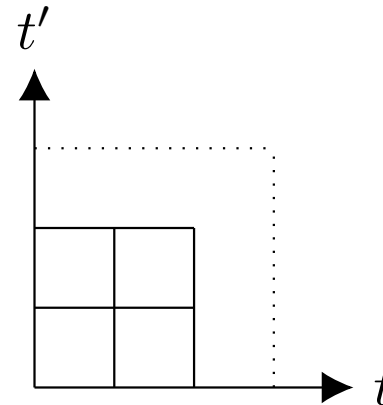
effective mass

Numerical solution of the equations of motion

- symmetries: spatial homogeneity & isotropy
- propagator decomposition:

$$G(x, y) = \underbrace{F(x, y)}_{\text{statistical function}} + \frac{i}{2} \underbrace{\rho(x, y)}_{\text{spectral function}} \operatorname{sgn}(x^0 - y^0)$$

- iterative real-time evolution

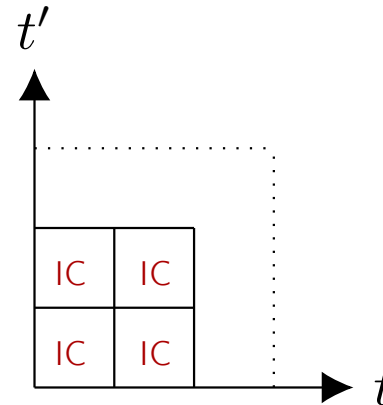


Numerical solution of the equations of motion

- symmetries: spatial homogeneity & isotropy
- propagator decomposition:

$$G(x, y) = \underbrace{F(x, y)}_{\text{statistical function}} + \frac{i}{2} \underbrace{\rho(x, y)}_{\text{spectral function}} \operatorname{sgn}(x^0 - y^0)$$

- iterative real-time evolution

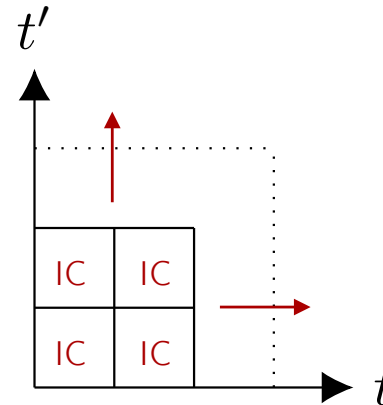


Numerical solution of the equations of motion

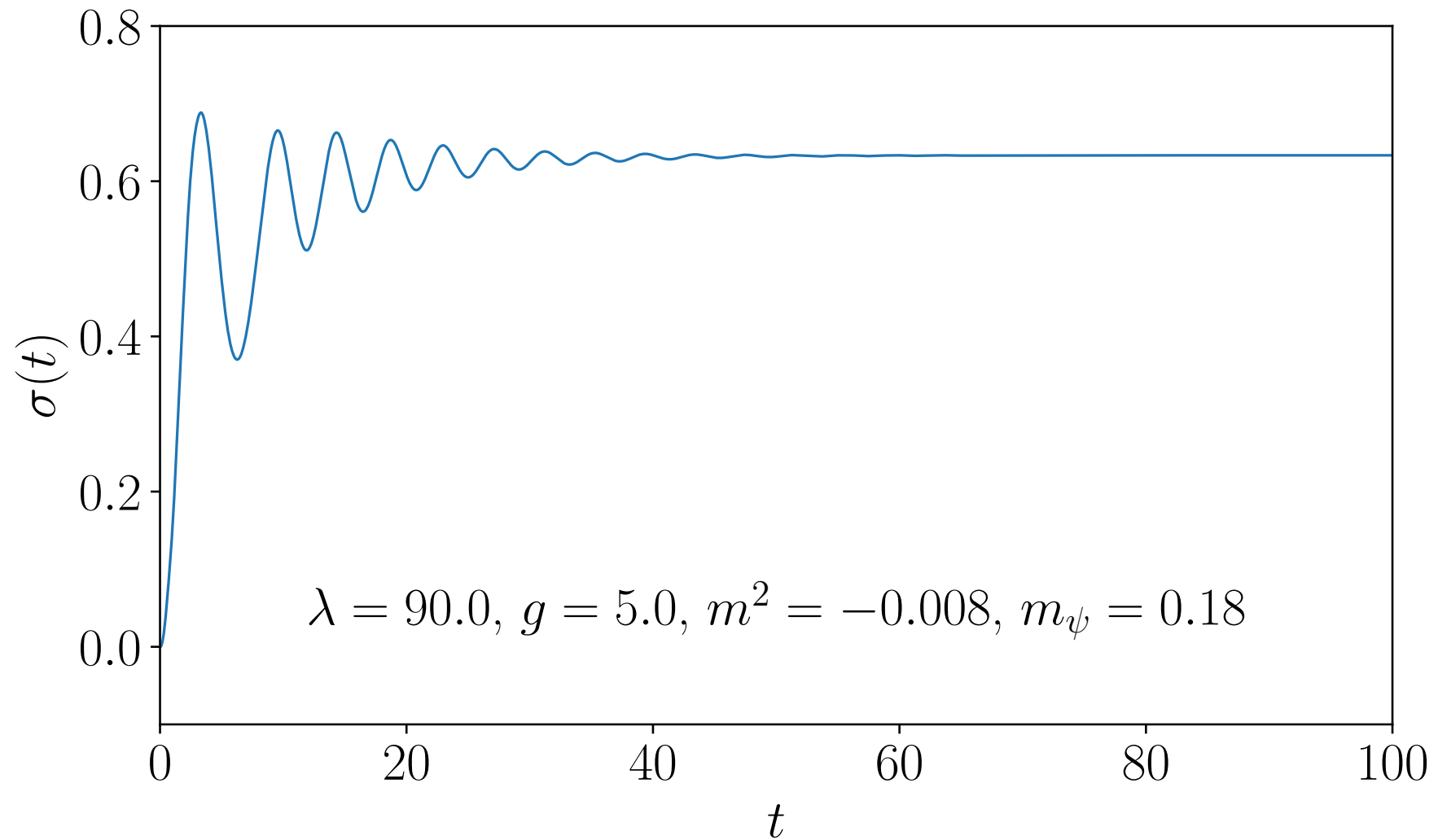
- symmetries: spatial homogeneity & isotropy
- propagator decomposition:

$$G(x, y) = \underbrace{F(x, y)}_{\text{statistical function}} + \frac{i}{2} \underbrace{\rho(x, y)}_{\text{spectral function}} \operatorname{sgn}(x^0 - y^0)$$

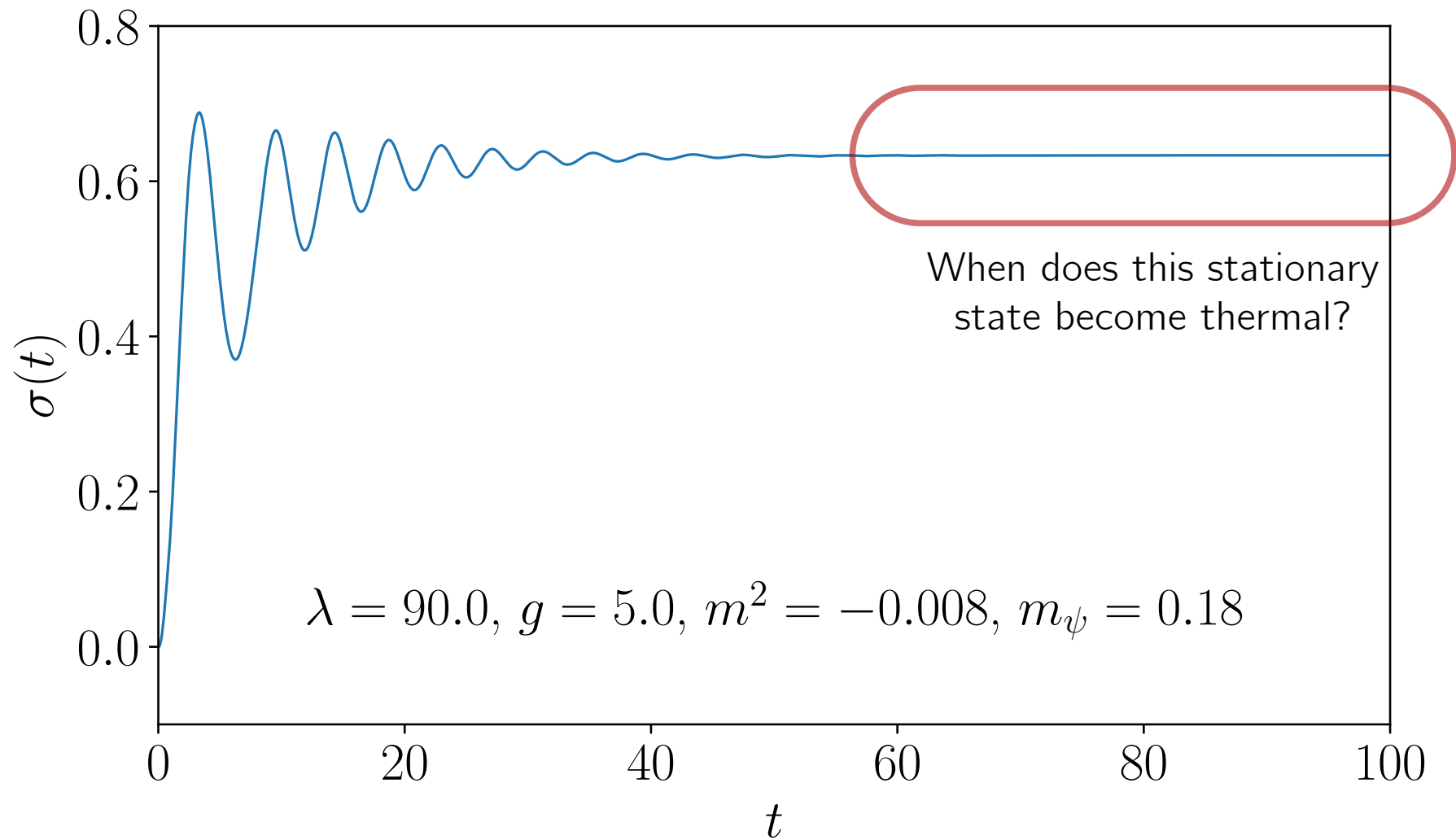
- iterative real-time evolution



Real-time evolution of the macroscopic field



Real-time evolution of the macroscopic field



(1) Thermal equilibrium is a time-translation invariant state.

- time-translation invariance implies

$$G(t, t', |\mathbf{p}|) \rightsquigarrow G(\omega, |\mathbf{p}|)$$

in general depending
on $t + t'$ and $t - t'$

independent of $t + t'$
here is something

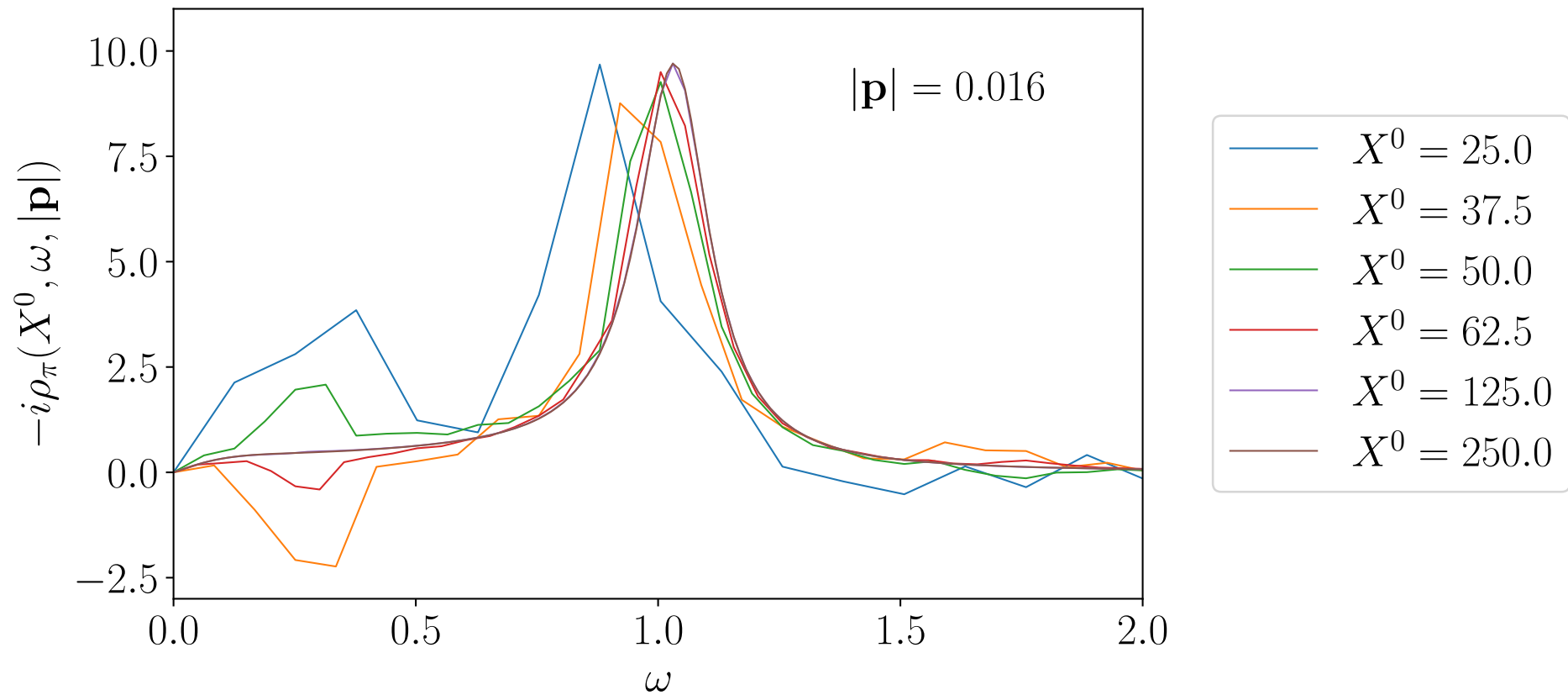
- temporal Wigner transformation:

$$\rho(t, t', |\mathbf{p}|) \rightarrow \rho(X^0, \omega, |\mathbf{p}|)$$

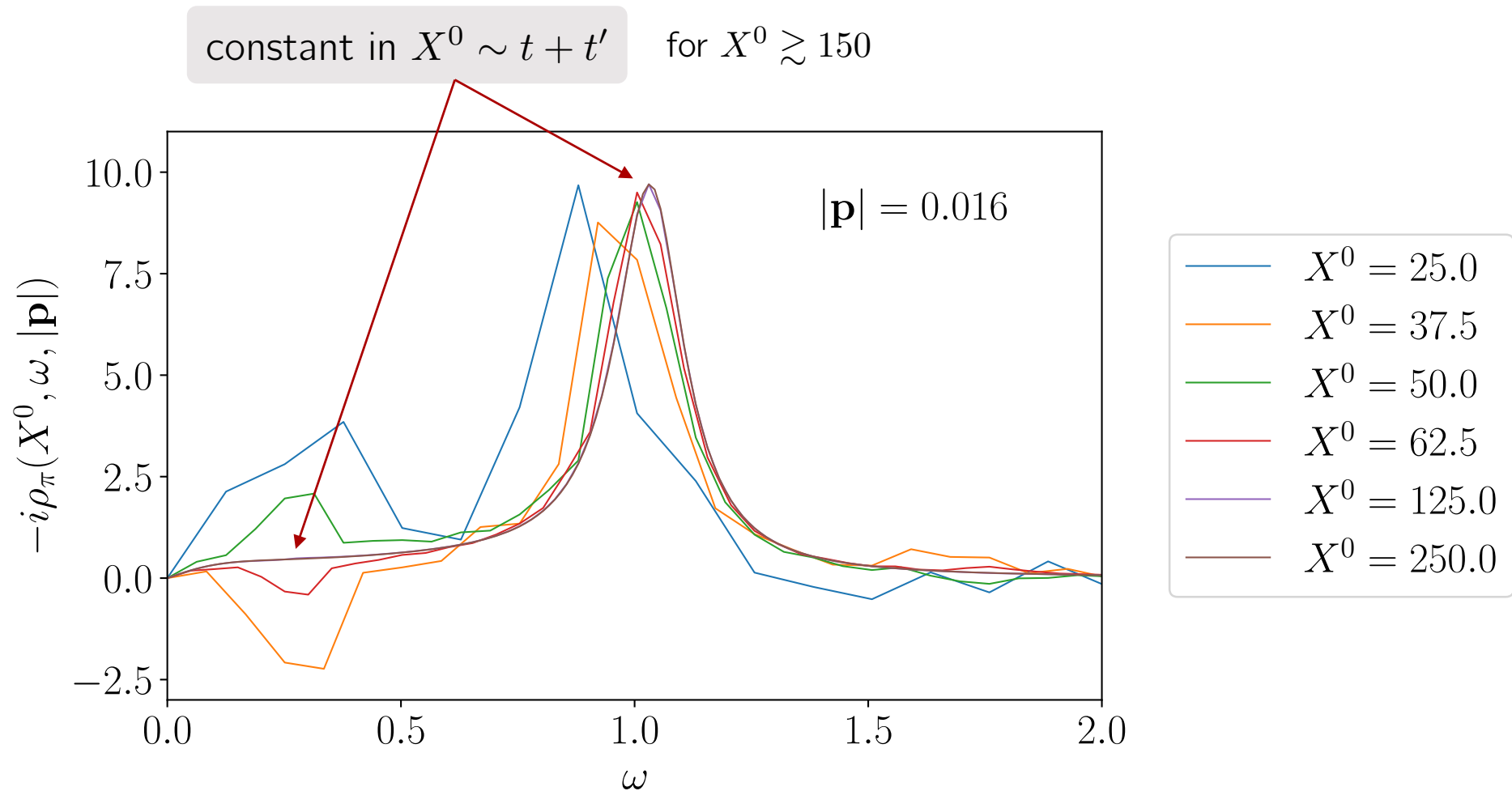
center-of-mass time
 $X^0 = \frac{t+t'}{2}$

frequency
 $X^0 = \frac{t+t'}{2}$

The two-point functions become time-translation invariant.



The two-point functions become time-translation invariant.



(2) Thermal eq. as state with thermal particle distributions.

- thermal initial density matrix implies fluctuation-dissipation relation:

$$F_{\text{eq}}(\omega, |\mathbf{p}|) = -i \left(\frac{1}{2} + n_{\text{th}}(\omega) \right) \rho_{\text{eq}}(\omega, |\mathbf{p}|)$$

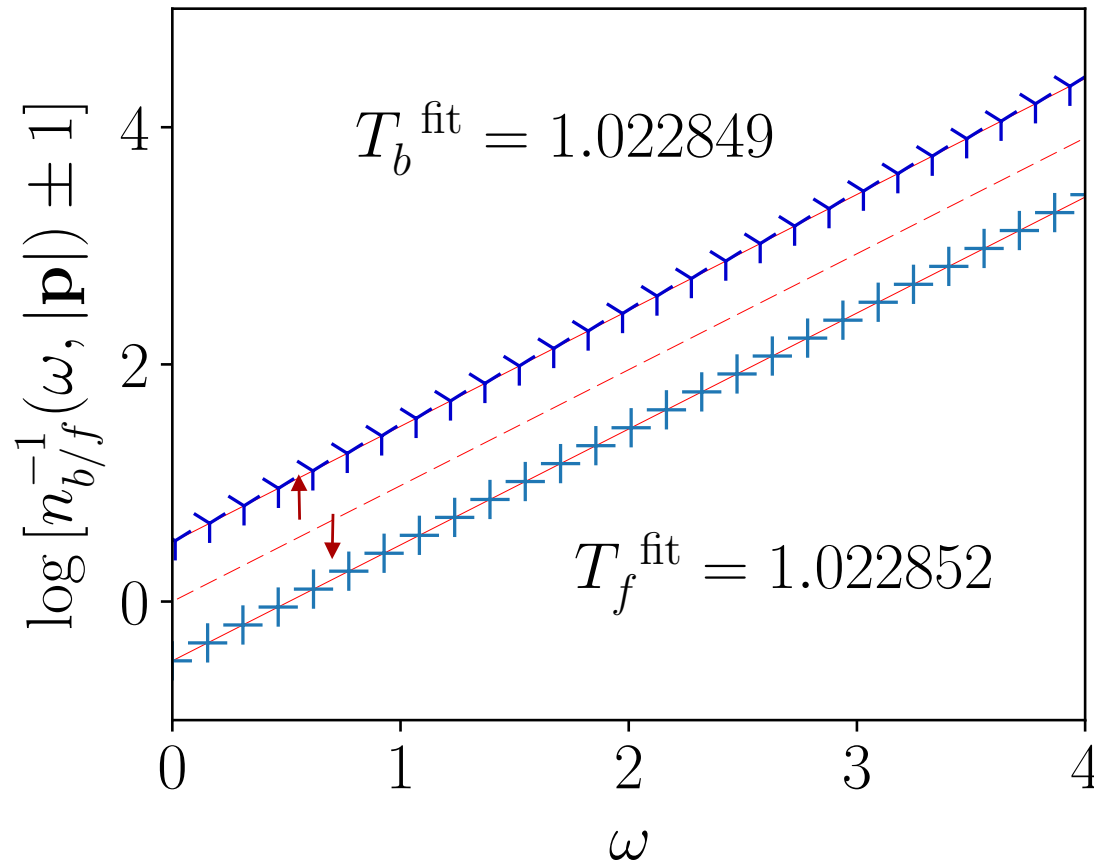
- effective particle number:

$$n(\omega, |\mathbf{p}|) = i \frac{F(\omega, |\mathbf{p}|)}{\rho(\omega, |\mathbf{p}|)} - \frac{1}{2}$$

- in thermal equilibrium:

$$n(\omega, |\mathbf{p}|) \rightarrow n_{\text{BE/FD}}(\omega) = \frac{1}{e^{\beta\omega} \mp 1} \text{ with } \beta = 1/T$$

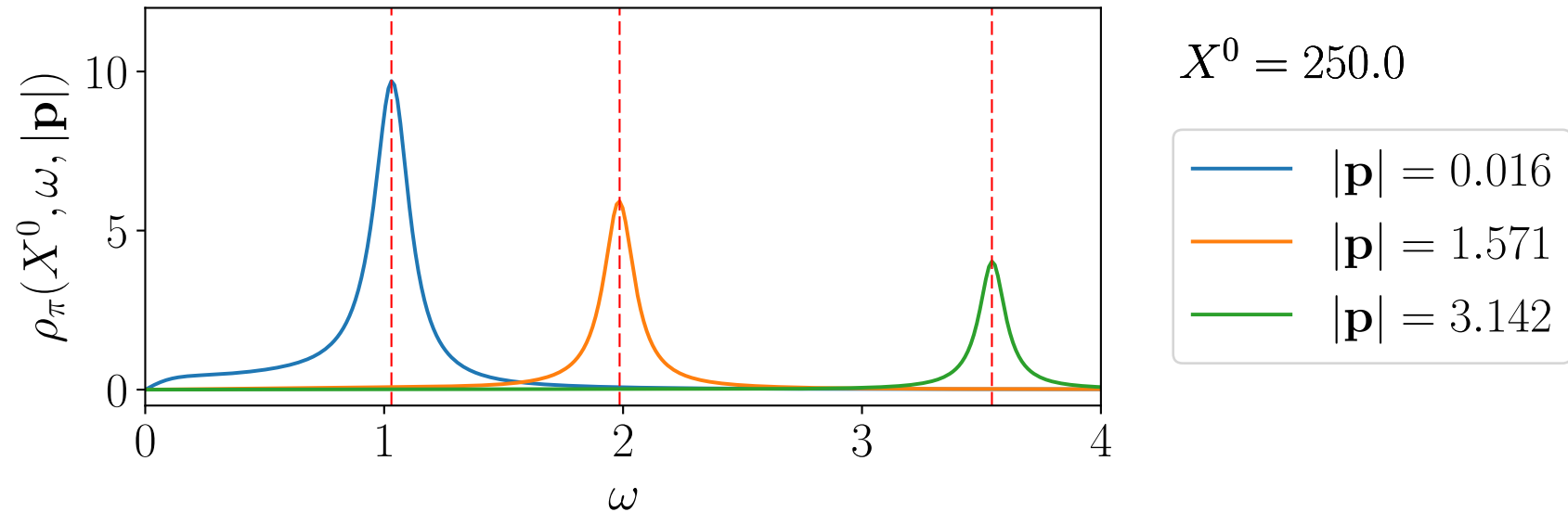
Determination of the thermalization temperature using the Bose-Einstein and Fermi-Dirac distribution



Y boson (pion)
+ fermion

$$T \approx m_\pi \approx 130 \text{ MeV}$$

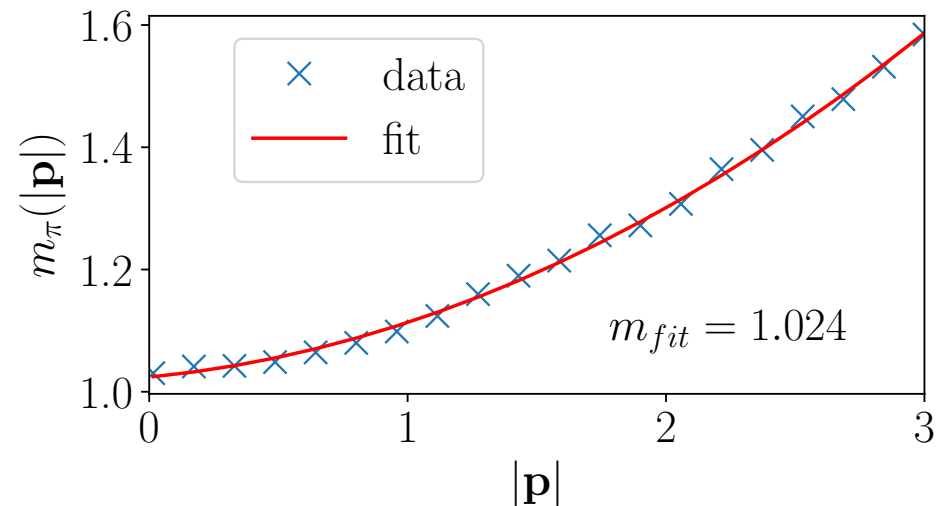
Particle masses from spectral functions by dispersion relation



- particle mass from peak position:

$$m(|\mathbf{p}|) = \sqrt{\omega_{\text{peak}}^2(|\mathbf{p}|^2) - |\mathbf{p}|^2}$$

- physical mass at zero momentum



A step forward in describing the thermalizing of the QGP in a heavy ion collision

We were able to

- include non-equilibrium dynamics
- observe the approach of thermal equilibrium
- determine the physical mass spectrum

Next steps:

- non-zero baryon-chemical potential
- expanding box size
- scaling behavior around critical point